Conference materials
UDC 537
DOI: https://doi.org/10.18721/JPM.163.272

# Hardware- and user-induced micromobility effects in in-door radio access at 140 GHz

T.A. Yaropolov[1]✉, A.N. Prikhodko[1,2], P.V. Rozhkova[1], A.S. Shurakov[1,2], G.N. Goltsman[1,2]

[1] Moscow Pedagogical State University, Moscow, Russia;

[2] National Research University Higher School of Economics, Moscow, Russia

✉ yaropolov.26012001@yandex.ru

**Abstract.** Sub-terahertz frequency band is beneficial for radio access networks of the sixth generation. Due to rather limited power capacity, there appears a necessity to equip transmitters and receivers in sub-terahertz wireless channels with high directivity antennas. This, however, leads to a potential connection failure in response to even a minor linear or angular displacement of a user equipment. This article is focused on a hardware- and user-induced micromobility effects for different scenarios of in-door radio access at carrier frequency of 140 GHz. The developed measurement setup enables fast simultaneous logging of linear and angular displacements of a user equipment with respect to radio access point and the corresponding received signal strength. Experimental data is processed by Allan variance analysis, statistics is acquired for a large number of samples. We believe that our findings should be of use in the development of beam steering solutions for reliable sub-terahertz wireless communications.

**Keywords:** user micromobility, 6G wireless system, sub-terahertz communication

**Funding:** Hardware development was conducted as a part of strategic project "Digital Transformation: Technologies, Effectiveness, Efficiency" of Higher School of Economics development programme granted by Ministry of science and higher education of Russia "Priority-2030" grant as a part of "Science and Universities" national project. Data processing was partly funded by the Russian Science Foundation grant 22-79-10279, https://rscf.ru/project/22-79-10279/.

**Citation:** Yaropolov T.A., Prikhodko A.N., Rozhkova P.V., Shurakov A.S., Goltsman G.N., Hardware- and User-Induced Micromobility Effects in In-Door Radio Access at 140 GHz, St. Petersburg State Polytechnical University Journal. Physics and Mathematics. 16 (3.2) (2023) 411–416. DOI: https://doi.org/10.18721/JPM.163.272

Материалы конференции
УДК 537
DOI: https://doi.org/10.18721/JPM.163.272

# Аппаратный и пользовательский вклад в эффект микромобильности при радиодоступе на 140 ГГц внутри помещений

Т.А. Ярополов[1]✉, А.Н. Приходько[1,2], П.В. Рожкова[1], А.С. Шураков[1,2], Г.Н. Гольцман[1,2]

[1] Московский Педагогический Государственный Университет, Москва, Россия;

[2] Национальный исследовательский университет «Высшая школа экономики», Москва, Россия

✉ yaropolov.26012001@yandex.ru

**Аннотация.** Суб-терагерцовый диапазон частот привлекателен для сетей радиодоступа шестого поколения. Ограниченность уровня доступной мощности приводит к необходимости оснащения передатчиков и приемников в суб-терагерцовых беспроводных каналах связи сверхузконаправленными антеннами. Это, в свою очередь, способно приводить к разрыву соединения даже при незначительных линейных или угловых смещениях пользовательского устройства. Данная статья посвящена исследованию аппаратного и пользовательского вклада в эффект микромобильности при радиодоступе на несущей частоте 140 ГГц внутри помещений. Разработанная измерительная установка обеспечивает возможность быстрой записи линейных и угловых перемещений пользовательского устройства относительно точки радиодоступа и соответствующего уровня принимаемого сигнала. Статистический анализ экспериментальных данных осуществляется с использованием кривой дисперсии Аллана для большой выборки измерений. Мы полагаем, что наши результаты могут быть использованы при разработке устройств управления пучком в суб-терагерцовой беспроводной связи повышенной надежности.

**Ключевые слова:** микромобильность пользователя, беспроводная система 6G, суб-терагерцовая связь

**Финансирование:** Разработка аппаратного обеспечения подготовлена в ходе реализации стратегического проекта «Цифровая трансформация: технологии, эффекты, эффективность» программы развития национального исследовательского университета «Высшая школа экономики» в рамках участия в программе Минобрнауки России «Приоритет-2030» национального проекта «Наука и университеты». Обработка данных частично выполнена за счет гранта Российского научного фонда № 22-79-10279, https://rscf.ru/project/22-79-10279/.

**Ссылка при цитировании:** Ярополов Т.А., Приходько А.Н., Рожкова П.В., Шураков А.С., Гольцман Г.Н. Аппаратный и пользовательский вклад в эффект микромобильности при радиодоступе на 140 ГГц внутри помещений // Научно-технические ведомости СПбГПУ. Физико-математические науки. 2023. Т. 16. № 3.2. С. 411–416. DOI: https://doi.org/10.18721/JPM.163.272



## Introduction

Sub-terahertz frequency (sub-THz) band is beneficial for wireless radio access networks of the sixth generation (6G). It is conventionally proposed to use highly directive antennas in transmitters ($T_x$) of access points and receivers ($R_x$) of user equipment (UE) in 6G networks. In this case, reliability of wireless channel can be notably compromised if UE is mobile. User micromobility is one of the main issues in the implementation of 6G wireless communication systems [1, 2]. In this work, we study hardware- and user-induced micromobility effects for different scenarios

of in-door radio access at carrier frequency of 140 GHz. The considered scenarios are mainly related to web searching and online gaming characterized by low-deterministic misalignment between sub-THz beams of $T_x$ and $R_x$. We develop measurement setup for fast simultaneous logging of time-dependent position of UE with respect to $T_x$ and the corresponding signal strength at $R_x$. Time related metrics are statistically acquired by Allan variance analysis. In addition, our measurements enable profiling of the $R_x$ signal strength in different $T_x$ beam planes. This should find use in the development of beamforming solutions for 6G wireless communication systems.

## Materials and Methods

We fabricate UE with linear dimensions similar to a typical large-screen smartphone to insure its realistic mechanics in user hands. UE is equipped with a motion sensor and $R_x$ and is placed far behind a Fraunhofer distance in front of $T_x$. The sensor makes use of microelectromechanical system (MEMS) accelerometers and gyroscopes and measures linear accelerations and angular velocities with respect to 3-dimensional intrinsic reference frame (IRF). Referring to Fig. 1,*a*, the angles φ and θ are restored in the spherical coordinate system fixed to UE. They are defined as the angles between the corresponding axes of IRF at the initial moment of time $t = 0$ ($x(0)$ and $z(0)$) and during current measurement (x(t) and z(t)). The measurements are carried out with $T_x$ providing a constant waveform signal at carrier frequency of 140 GHz and an amplitude modulation at 25 kHz. $R_x$ is based on a waveguide Schottky diode envelope detector [2]. The readout is maintained by a selective nanovoltmeter. The detector response voltage, i.e., signal strength at $R_x$, is recorded simultaneously with the readings of accelerometers and gyroscopes by a data acquisition system. This ensures an exact correspondence of the changes in the received signal strength with the UE angular coordinates.

As shown in Fig. 1,*b*, antennas of $T_x$ and $R_x$ have far-field beamwidths of 6–17°. We subsequently use a pair of diagonal horn antennas with bigger (Horn 1) and less directivity (Horn 2) to distinguish between the beamwidth and polarization impacts on signal attenuation upon user micromobility. Schematic diagram of the measurement setup developed for the empirical studies is presented in Fig. 2. The $R_x$ unit utilizes a membrane-integrated Schottky diode detector [3] and a 16-bit motion sensor [4] enabling simultaneous logging of 3 linear accelerations ($a_x$, $a_y$, $a_z$) and 3 angular velocities ($\omega_x$, $\omega_y$, $\omega_z$). Quaternion math and Mahony complementary filter are used for fast (on a millisecond scale) and precise position measurements of the motion sensor.

To ensure reliability and reproducibility of the position measurement of $R_x$ with respect to the $T_x$ beam, we perform a series of calibrations for different initial orientations of $R_x$ (i.e., for different initial orientations of the motion sensor IRF). Tables 1 and 2 contain statistics on the triplets of linear accelerations and angular velocities measured for static $R_x$, when its different planes (see Fig. 1,*a*) are set parallel to the horizon.

After achieving the appropriate performance of the measurement setup, we further decide to conduct a series of independent measurements of a signal strength at $R_x$ as a function of its angular position with respect to the $T_x$ beam for different radio access scenarios in 6G networks.

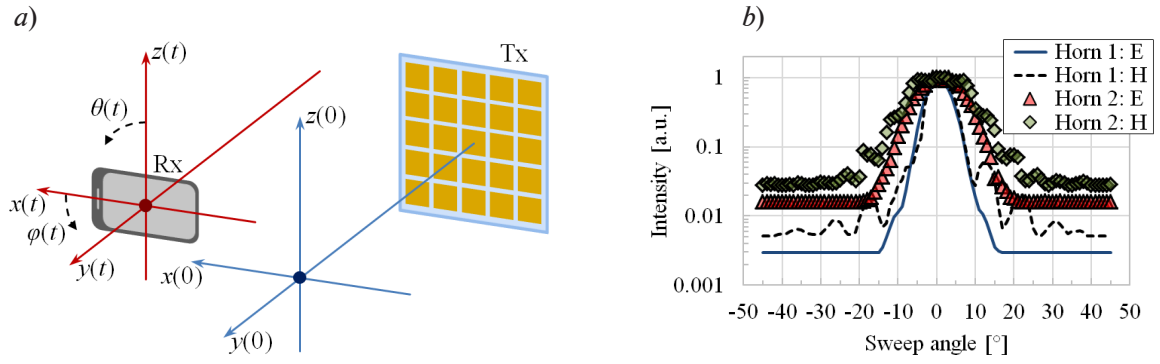


Fig. 1. Wireless channel with static sub-THz access point and mobile UE (*a*). *E*- and *H*- plane beam profiles of 2 alternatively employed $T_x/R_x$ horn antennas (*b*)

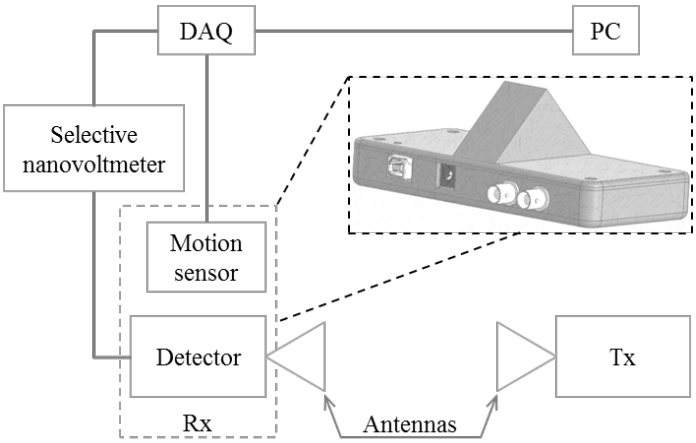


Fig. 2. Measurement setup developed for empirical studies of user micromobility at 140 GHz

Table 1

**Statistics on linear accelerations for a set of 10 time series with up to 45000 readings logged for a static $R_x$ with different orientations of the motion sensor IRF**

| IRF orientation | Statistics on linear accelerations | | |
|---|---|---|---|
| | $\langle a_x \rangle_{avg} \pm \Delta a_x$, m/s$^2$ | $\langle a_y \rangle_{avg} \pm \Delta a_y$, m/s$^2$ | $\langle a_z \rangle_{avg} \pm \Delta a_z$, m/s$^2$ |
| XOY | 0.002±0.002 | −0.002±0.001 | −0.001±0.009 |
| XOZ | 0.02±0.17 | −0.01±0.04 | −0.08±0.19 |
| YOZ | −0.03±0.15 | 0.06±0.08 | −0.17±0.05 |

Notations: Here $\langle a_x \rangle_{avg}$, $\langle a_y \rangle_{avg}$, $\langle a_z \rangle_{avg}$ are the average values of mean linear accelerations along the $x$-, $y$-, $z$-axes of the motion sensor IRF and $\Delta a_x$, $\Delta a_y$, $\Delta a_z$ are the corresponding confidence intervals.

Table 2

**Statistics on angular velocities for a set of 10 time series with up to 45000 readings logged for a static $R_x$ with different orientations of the motion sensor IRF**

| IRF orientation | Statistics on angular velocities | | |
|---|---|---|---|
| | $\langle \omega_x \rangle_{avg} \pm \Delta\omega_x$, rad/s | $\langle \omega_y \rangle_{avg} \pm \Delta\omega_y$, rad/s | $\langle \omega_z \rangle_{avg} \pm \Delta\omega_z$, rad/s |
| XOY | −6.5e-5±3.6e−5 | −6.3e-5±3.0e−5 | −5.4e-5±4.5e−5 |
| XOZ | −6.4e-5±3.4e−5 | −5.8e-5±1.0e−5 | −5.8e-5±2.8e−5 |
| YOZ | −6.3e-5±1.1e−5 | −5.9e-5±1.5e−5 | −6.3e-5±1.7e−5 |

Notations: Here $\langle \omega_x \rangle_{avg}$, $\langle \omega_y \rangle_{avg}$, $\langle \omega_z \rangle_{avg}$ are the average values of mean angular velocities along the $x$-, $y$-, $z$-axes of the motion sensor IRF and $\Delta\omega_x$, $\Delta\omega_y$, $\Delta\omega_z$ are the corresponding confidence intervals.

## Results and Discussion

As a first measurement of interest, we choose the scenario of an incoming phone call to a person working at the office desk. In this scenario, UE (i.e., $R_x$) is initially put on the desk, optical axis of $R_x$ horn antenna is coaligned with that of $T_x$ placed 1.5 m away. Polarization planes of the antennas are also coaligned. UE is in the hand of a user moving it from the desk to his ear, the

elbow does not leave the desk surface upon the move. Thus, 2 key effects are presented: gradual change of the angle between the polarization planes of the $T_x$ and $R_x$ horn antennas from 0 to 90° and spontaneous changes in the orientation of the $R_x$ horn antenna optical axis induced by the human mechanics. We carry out 2 series of 10 independent measurements for the considered scenario. Statistically processed results of the measurements for 2 pairs of $T_x/R_x$ pyramidal horn antennas with bigger (Horn 1) and less directivity (Horn 2) are provided in Fig. 3,*a*. The figure contains smoothed mean signal strengths at $R_x$ with 68% confidence intervals for different values of angle θ. We employ a moving average with a window size of 178 samples to get a 3° resolution upon smoothing. Using this empirical data together with Malus's law, one can distinguish between the beamwidth and polarization impacts on signal attenuation upon user micromobility in a phone call scenario.

We further employ the developed measurement setup to study stability of the received signal upon a short distance transmission for online gaming and web searching scenarios. During the online gaming scenario, the user pretends to play an arcade racing game on a UE tilted forward at 45° with respect to the vertical in his hands. The wide side of the UE is oriented horizontally. The web searching scenario focuses on the user mechanics in the process of using the search engine in the UE browser. The orientation of the UE in the hands of the user is the same as during the online gaming scenario. In both scenarios, the user stands still and taps on the UE screen inducing its angular displacements followed by changes in the signal strength at $R_x$. To analyze the signature of application-dependent mechanics, a series of up to 100 independent measurements with a duration of 60 s each is conducted. At the beginning of each measurement, optical axis and polarization plane of $R_x$ horn antenna are coaligned with those of $T_x$ placed 1.5 m away. The experimental data is statistically processed by Allan variance analysis [5]. Fig. 3,*b* summarizes results of the processing, stability of the received signal for a static position of UE at the initial moment of time $t = 0$ is provided as a reference. The latter obeys a radiometer equation for integration times, τ, from 2 ms to 2 s. This ensures reliable extraction of the micromobility-induced instabilities in the received signal. For online gaming scenario, we observe white noise and drift signatures for τ of below and above 4 ms, respectively. No $1/F$-noise signature is recognized. Furthermore, confidence intervals for the Allan variance values widen with increase in τ. And they are notably wider as compared to the web searching curve at any given τ. For web searching scenario, we observe $1/F$-noise and drift signatures for τ of below and above 4 ms, respectively. No pronounced white noise signature is recognized. The acquired Allan variance curves also reveal high repeatability in numerous independent measurements. Moreover, the developed measurement setup enables stability profiling for a number of planes with respect to the $T_x$ beam. This aids to analyze contribution of UE optics design and user activity to the received signal stability. Further detailed studies of the mutual impact of user micromobility and dynamic blockages [6] on connection quality in sub-terahertz communications are in our future plans. However, we believe that the reported results should find use in the development of efficient beam steering solutions for reliable sub-terahertz wireless communication systems.

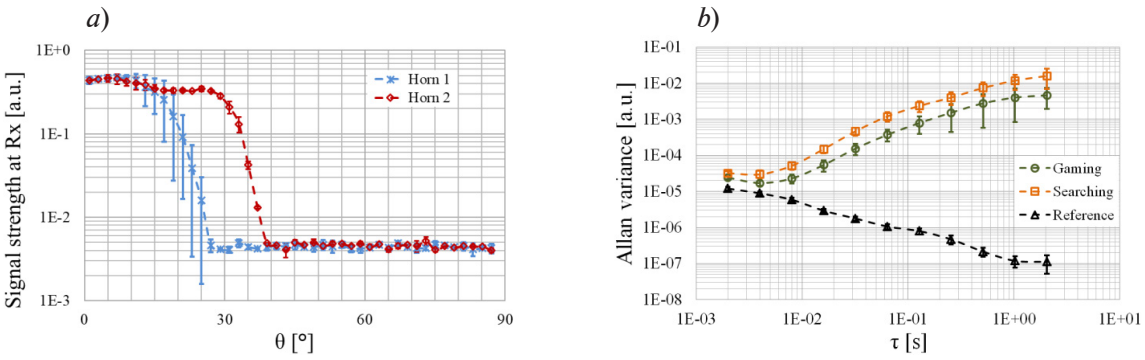


Fig. 3. Signal strength at UE measured for user micromobility during a phone call (*a*). Experimental Allan variance curves for signal strength at UE in various application scenarios (*b*)

## Conclusion

To study user micromobility for different radio access scenarios in 6G networks, we fabricate UE with linear dimensions similar to a typical large-screen smartphone to insure its realistic mechanics in user hands. UE is equipped with a motion sensor and $R_x$ and is placed far behind a Fraunhofer distance in front of $T_x$. The motion sensor is a MEMS-based multi-channel logging device combined with quaternion math and Mahony complementary filter for fast (on a millisecond scale) and precise position measurements. Antennas of $T_x$ and $R_x$ have far-field beamwidths of 6–17° similar to those expected for first-run wireless 6G systems. The measurements of a signal strength at $R_x$ in user hands are carried out with $T_x$ providing a constant waveform signal at carrier frequency of 140 GHz and an amplitude modulation at 25 kHz. The experimental data is statistically processed by Allan variance analysis for the considered gaming and web searching scenarios. The developed measurement setup enables stability profiling for a number of planes with respect to the $T_x$ beam. This aids to analyze contribution of UE optics design and user activity to the received signal stability. We believe that the reported results should find use in the development of efficient beam steering solutions for reliable sub-terahertz wireless communication systems.

## REFERENCES

1. **Petrov V., Moltchanov D., Koucheryavy Y., Jornet J.M.,** Capacity and outage of terahertz communications with user micro-mobility and beam misalignment, IEEE Transactions on Vehicular Technology. 69 (4) (2020) 6822–6827.

2. **Stepanov N., Moltchanov D., Begishev V., Turlikov A., Koucheryavy Y.,** Statistical analysis and modeling of user micromobility for THz cellular communications, IEEE Transactions on Vehicular Technology. 71 (1) (2021) 725–738.

3. **Shurakov A., Belikov I., Prikhodko A., Mikhailov D., Gol'tsman G.,** Membrane-integrated planar Schottky diodes for waveguide mm-Wave detectors, Microwave & Telecommunication Technology. 3 (2021) 34.

4. TDK InvenSense. URL: https://invensense.tdk.com/products/motion-tracking/6-axis/mpu-6500/.

5. **Allan D. W.,** Statistics of atomic frequency standards, Proceedings of the IEEE. 54 (2) (1966) 221–230.

6. **Shurakov A., Moltchanov D., Prikhodko A., Khakimov A., Mokrov E., Begishev V., Belikov I., Koucheryavy Y., Gol'tsman G.,** Empirical blockage characterization and detection in indoor sub-THz communications, Computer Communications. 201 (2023) 48–58.

## THE AUTHORS

**YAROPOLOV Terentiy A.**
yaropolov.26012001@yandex.ru
ORCID: 0000-0001-9521-9651

**SHURAKOV Alexander S.**
alexander@rplab.ru
ORCID: 0000-0002-4671-7731

**PRIKHODKO Anatoliy N.**
anatprikh1995@yandex.ru
ORCID: 0000-0002-4859-8975

**GOLTSMAN Grigory N.**
goltsman@rplab.ru
ORCID: 0000-0002-1960-9161

**ROZHKOVA Polina V.**
pv_rozhkova2@student.mpgu.edu
ORCID: 0009-0005-6258-9353

*Received 21.07.2023. Approved after reviewing 06.09.2023. Accepted 07.09.2023.*